

pubs.acs.org/journal/ascecg Research Article

High-Performance Ether-Free Poly(terphenyl-co-9,9-dimethylfluorene-ethylimidazole) Membranes for High Temperature Proton Exchange Membrane Fuel Cells

Lei Li, Qi Liao, Ruixuan Lv, Lele Wang, Lili Sui, Jin Wang,* and Jingshuai Yang*



Cite This: ACS Sustainable Chem. Eng. 2025, 13, 13656-13666



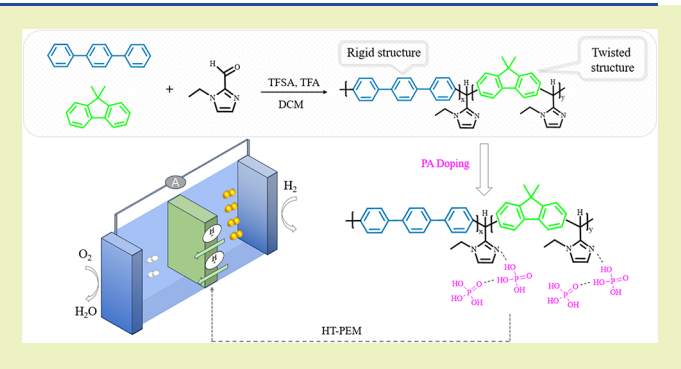
ACCESS I

Metrics & More

Article Recommendations

SI Supporting Information

ABSTRACT: High-temperature proton exchange membranes (HT-PEMs) are essential components in HT-PEM fuel cells. Although phosphoric acid (PA)-doped polybenzimidazole (PBI) membranes are widely used, the development of HT-PEMs that are more cost-effective, easier to synthesize, and offer enhanced physicochemical performance remains a critical research focus. In this study, we report a new class of ether-free poly(terphenyl-co-9,9'-dimethylfluorene-ethylimidazole) copolymers synthesized via a superacid-catalyzed Friedel—Crafts hydroxyalkylation reaction. Rigid p-terphenyl (TP) and sterically twisted 9,9'-dimethylfluorene (DMF) segments were systematically copolymerized with 1-ethyl-2-imidazolecarbaldehyde (EtIm) to modulate the polymer back-



bone architecture and membrane performance. The incorporation of DMF units significantly enhances acid doping capacity and proton conductivity while maintaining good mechanical integrity. Among the copolymers, the optimized P(75%TP-25%DMF-EtIm) membrane achieves an acid doping content of 201%, a high proton conductivity of 124 mS cm⁻¹ at 180 °C, and a tensile strength of 6.02 MPa. When applied in an H_2 – O_2 fuel cell under anhydrous conditions and without backpressure, this membrane delivers an impressive peak power density of 1060 mW cm⁻² at 200 °C. These results demonstrate the great promise of ether-free P(x%TP-y% DMF-EtIm) based copolymers as next-generation HT-PEMs, offering a compelling alternative to conventional PBI membranes for high-performance fuel cell applications.

KEYWORDS: poly(terphenyl-co-9,9'-dimethylfluorene-ethylimidazole), copolymer, ether-free polymer, high temperature proton exchange membrane, fuel cell

1. INTRODUCTION

In light of growing environmental concerns and the depletion of fossil fuels, proton exchange membrane fuel cells (PEMFCs) have emerged as a promising clean energy technology due to their high power density and zero carbon emissions. Among them, high temperature PEMFCs (HT-PEMFCs), operating in the range of 120-200 °C, offer additional advantages such as simplified water management, accelerated electrode kinetics, and improved CO tolerance. 1,2 The core component of HT-PEMFCs is the high temperature proton exchange membrane (HT-PEM), which enables proton conduction and separates the electrodes under elevated temperatures.²⁻⁴ To date, phosphoric acid (PA) doped polybenzimidazole (PBI) membranes have been widely regarded as state-of-the-art HT-PEMs due to their excellent thermal and mechanical stability.3-8 The abundant benzimidazole units in the PBI backbone can form stable acid—base complexes with PA, contributing to high proton conductivity. 9 To address the poor solubility of high-molecular-weight PBI in organic solvents and to eliminate the use of such solvents in the conventional imbibing process, the polyphosphoric acid (PPA) method was

developed by Murdock and Benicewicz.⁶ This process, which has been commercialized by BASF in the form of Celtec membranes, enables the fabrication of PA doped PBI membranes with excellent electrochemical performance.^{3,10} Nevertheless, the continued development of novel HT-PEMs with enhanced performance, reduced toxicity, and improved processability remains critically important.

In recent years, various alternative polymers bearing basic functional groups have been explored for HT-PEM applications. These groups can interact with PA through hydrogen bonding, thereby forming continuous proton conduction networks. Among them, polymers containing quaternary ammonium (QA) or imidazole/imidazolium moieties have

Received: June 23, 2025 Revised: July 30, 2025 Accepted: July 30, 2025 Published: August 12, 2025





Figure 1. Synthesis of P(x%TP-y%DMF-EtIm) copolymers.

shown great promise due to their strong PA affinity and high conductivity. ^{11–14} Particularly, imidazole-functionalized polymers offer abundant proton transfer sites and robust hydrogen bonding with PA, enabling high temperature operation. ^{11,13,15,16} As a widely used strategy, side-chain imidazolium groups are typically grafted onto poly(arylene ether sulfone/ketone) backbones via halomethylation followed by the Menshutkin reaction. However, such membranes often suffer from limited mechanical and chemical stability. ^{13,17}

Main-chain incorporation of N-heterocyclic units into aromatic polymer backbones has attracted increasing attention due to the resulting enhancement in thermal stability, chemical resistance, and mechanical robustness. Recently, one efficient method to construct rigid wholly aromatic polymers is the metal-free, one-pot Friedel-Crafts hydroxyalkylation reaction between electron-rich arenes and aldehydes or ketones, catalyzed by superacids. as exemplified by Zolotukhin et al. 18,19 Regarding polymer electrolyte membranes, this method was first applied to the synthesis of poly(arylene piperidine) (PAP) membranes for use in anion exchange membranes (AEMs).²⁰⁻²² Owing to the suppression of Hofmann elimination, the resulting quaternized PAP based AEMs exhibited improved alkaline stability along with high ionic conductivity.²⁰ Inspired by these findings, a variety of aromatic polymers incorporating piperidine^{23–25} and pyridine^{26–30} units have since been developed and investigated for application in HT-PEMs. Building on these advances, our group previously reported imidazole-functionalized polymers prepared via Friedel—Crafts polycondensation using 1-methyl-2-imidazole-carbaldehyde. 31-33 These materials exhibited high PA uptake and excellent chemical durability owing to the enhanced basicity of the imidazole ring and the fully carbon-based backbones.

Although extensive research has been conducted on polymers with simple aromatic backbones such as *p*-terphenyl and biphenyl, copolymerization strategies offer greater structural flexibility and tunable properties by incorporating diverse monomer functionalities. ^{10,20,30,32–34} For instance, our group has systematically investigated how different backbone architectures, i.e., rigid, flexible, and bulky, affect the performance of pyridine-based HT-PEMs. ²⁸ Among these,

dibenzofuran is a rigid and planar unit characterized by extended conjugation and ether linkages, which provides multiple reactive sites and induces twisted polymer backbones with enlarged free volumes. 33,35-37 Likewise, 9,9-dimethylfluorene (DMF), a fluorene derivative with an almost zero dihedral angle, contributes significantly to backbone rigidity. ^{28,38,39} For example, Lee et al. integrated the rigid DMF unit into a copolymer (PFTP-13), which resulted in enhanced structural rigidity and a well-defined phase-separated morphology in the resulting AEMs, thereby improving both dimensional stability and ion conductivity.³⁸ An H₂-O₂ AEMFC assembled with the PFTP-13 membrane exhibited stable operation at 200 mA cm⁻² and 70 °C for approximately 200 h, with only a 3.68% voltage decay. Despite these promising features, DMF-based polymers have rarely been explored in HT-PEMFCs or incorporated into aldehyde-based copolymer systems, presenting a promising direction for future research and HT-PEM development.

In this work, we designed and synthesized a novel series of imidazole containing fully aromatic, ether-free copolymers incorporating p-terphenyl (TP) and DMF units, denoted as P(x%TP-y%DMF-EtIm), through a superacid-catalyzed onestep Friedel-Crafts hydroxyalkylation reaction using 1-ethyl-2imidazolecarbaldehyde (EtIm) as the functional monomer. The twisted DMF segment was expected to enhance backbone stiffness and disrupt polymer chain packing, leading to increased free volume and improved PA uptake. The use of a low-cost, highly reactive imidazole-based aldehyde monomer (EtIm) ensures efficient polymerization. By adjusting the TP/ DMF ratio, we systematically investigated the relationship between backbone architecture and membrane performance. The resulting PA doped membranes exhibited excellent thermal stability, high proton conductivity, and good fuel cell durability, demonstrating their potential as high-performance alternatives to conventional PBI-based HT-PEMs.

2. EXPERIMENTAL SECTION

2.1. Materials. *p*-Terphenyl (TP), 9,9-dimethylfluorene (DMF), 1-ethyl-2-imidazolecarbaldehyde (EtIm), and trifluoromethanesulfonic acid (TFSA) were purchased from Adamas Reagent Ltd. Dichloromethane (DCM), dimethylacetamide (DMAc), trifluoro-

Figure 2. Proposed reaction mechanism for synthesis of P(100%TP-EtIm).

acetic acid (TFA), phosphoric acid (85 wt %), and sodium bicarbonate (NaHCO $_3$) were obtained from Sinopharm Chemical Reagent Co., Ltd. All chemicals were used as received without further purification. The poly[2,2'-(p-oxidiphenylene)-5,5'-benzimidazole] (OPBI) was synthesized as described elsewhere.

2.2. Synthesis of Polymers. As illustrated in Figure 1, a series of copolymers were synthesized via a one-pot Friedel—Crafts hydroxyalkylation reaction catalyzed by TFSA. The reaction involved TP and DMF as aromatic units and EtIm as the electrophilic reagent. The molar ratio of the aldehyde to the total aromatic monomers was fixed at 110%. To investigate the influence of composition, three different feed ratios of TP to DMF were employed: 90:10, 75:25, and 60:40. The resulting copolymers were denoted as P(x%TP-y%DMF-EtIm), where x% and y% represent the molar ratios of TP and DMF, respectively, relative to EtIm.

Taking P(75%TP-25%DMF-EtIm) as an example, TP (1.52 g, 6.59 mmol), DMF (0.43 g, 2.19 mmol), and EtIm (1.17 g, 9.44 mmol) were added to a two-necked round-bottom flask, followed by the addition of 5 mL of DCM. The mixture was stirred in an ice bath for 10 min, after which TFA (0.3 mL) was added dropwise. The solution gradually turned white. Then, TFSA (7 mL) was slowly added, leading to a color change to gray. After stirring for 15 min, the ice bath was removed and the reaction proceeded at room temperature until a viscous dark-gray solution formed. The resulting product was precipitated into 1 M NaHCO3 solution, yielding a white polymer. The polymer was then cut into pieces and repeatedly washed with deionized water until the filtrate reached neutral pH. Finally, the product was dried in a vacuum oven at 80 °C for 12 h to obtain the final copolymer. In addition, both homopolymers including P(100% TP-EtIm) and P(100%DMF-EtIm) were synthesized as well as the reference polymers.

2.3. Preparation of Membranes. The membranes were prepared via the solution-casting method. Each synthesized copolymer was dissolved in DMAc (2 wt %) at 60 °C with continuous stirring to form a homogeneous solution. The solution was cast onto a clean, ultraflat dish and dried in a vacuum oven at 80 °C for 24 h to remove the solvent. After drying, the membranes were washed with deionized water and thoroughly dried again. The resulting membranes were uniform, flexible, and free of visible pores, with an average thickness of approximately 60 μ m.

2.4. Acid Doping and Swellings. The acid doping content (ADC%) and dimensional swelling behavior of the membranes were evaluated by measuring the mass, area, and volume of the membranes before and after PA doping. Membranes were immersed in 85 wt % PA at 30 °C for 48 h, until weight stabilization was achieved. Excess surface acid was gently removed using filter paper, followed by vacuum drying to eliminate absorbed water. ADC%, area swelling

ratio (AS%), and volume swelling ratio (VS%) were calculated using the following equations.

$$ADC\% = \frac{(m_{\rm PA} - m_{\rm dry})}{m_{\rm dry}} \times 100\% \tag{1}$$

$$AS\% = \frac{S_1 - S_0}{S_0} \times 100\% \tag{2}$$

$$VS\% = \frac{V_1 - V_0}{V_0} \times 100\% \tag{3}$$

In eq 1, $m_{\rm dry}$ and $m_{\rm PA}$ signify the membrane mass before and after PA doping, respectively. S_0 and S_1 refer to the membrane area prior to and subsequent to immersion in the PA solution, as per eq 2. Similarly, in accordance with eq 3, V_0 and V_1 represent the membrane volume before and after immersion in the PA solution.

2.5. Characterization. Inherent viscosities were determined using an Ubbelohde viscometer. Each copolymer was dissolved in DMAc at a concentration of 0.5 g dL $^{-1}$. Measurements were carried out at 25 °C, and inherent viscosities were calculated using the following equation

$$\eta = \frac{\ln(t_{\text{solution}}/t_{\text{DMAc}})}{c} \tag{4}$$

where $t_{\rm solution}$ and $t_{\rm DMAc}$ are the flow times of the polymer solution and pure DMAc solvent, respectively, and c is the concentration of the solution.

The molecular weight was measured through gel permeation chromatography (GPC) using Agilent GPC 50. The chemical structure of the polymers was confirmed by ¹H NMR spectroscopy using a Bruker Avance (600 MHz) spectrometer with tetramethylsilane (TMS) as the internal standard and DMSO- d_6 as the solvent. Fourier-transform infrared (FT-IR) spectra were recorded on a Bruker Vertex 70 spectrometer in the range of 4000-400 cm⁻¹. Membrane surface morphology was observed using a scanning electron microscope (SEM, Hitachi SU-8000) after sputter-coating with platinum. Thermal stability was assessed via thermogravimetric analysis (TGA) using a Rigaku TG/DTA8122 instrument under N₂ atmosphere, heating from 30 to 800 °C at a rate of 10 °C min⁻¹. Mechanical properties were evaluated using a CMT2000 tensile testing machine at room temperature, with a crosshead speed of 5 mm min⁻¹. Proton conductivity was measured using the four-probe AC impedance method, as described in our previous reports. ^{24,31} Prior to measurement, membranes were dried at 100 °C for 2 h to remove residual water. The proton conductivity (σ , S cm⁻¹) was calculated by eq 5

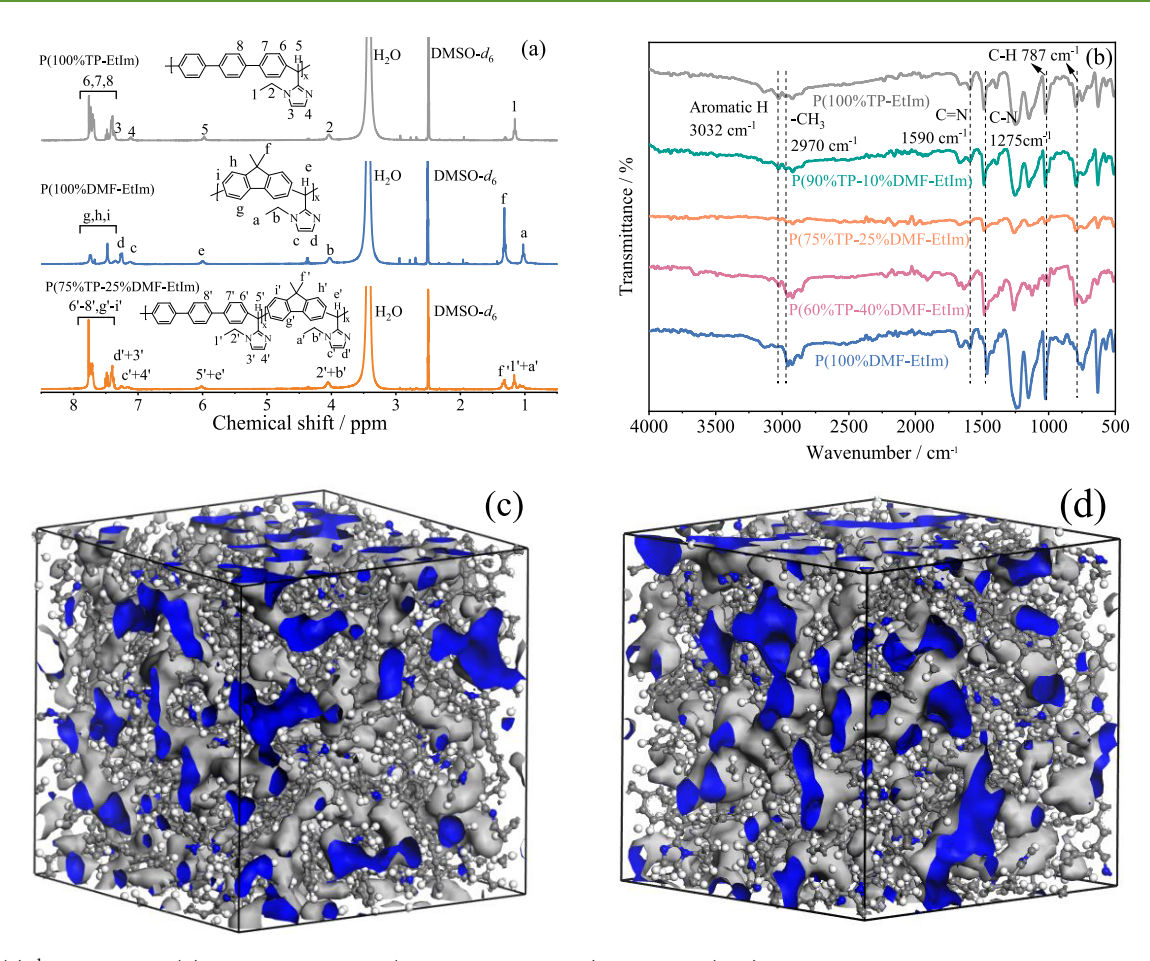


Figure 3. (a) 1 H NMR and (b) FT-IR spectra of P(x%TP-y%DMF-EtIm) polymers; (c, d) computational simulation structures of P(100%TP-EtIm) and P(100%DMF-EtIm) with accessible areas represented in blue.

$$\sigma = \frac{L}{RS} \tag{5}$$

where L is the distance between electrodes (cm), R is the membrane resistance (Ω) , W is the membrane width (cm), and T is the membrane thickness (cm).

Commercial gas diffusion electrodes (GDEs) were provided by Blue World Technologies. Pt/C and PtCo/C catalysts with a precious metal loading of 1.0 mg cm $^{-2}$ were used for anode and cathode, respectively. The membrane electrode assembly (MEA) was formed by hot pressing two GDEs onto both sides of the PA doped membrane at 110 °C and 25 kg cm $^{-2}$ for 1 min. Pure H₂ was fed to the anode at a flow rate of 50 mL min $^{-1}$ with a stoichiometric ratio (λ) of 1.8, while pure O₂ was supplied to the cathode at 30 mL min $^{-1}$ with a λ of 2.1. No backpressure or external humidification was applied during operation. The detail testing method was according to our previous work. 33

The electronic impedance spectroscopy (EIS) of the single cell was performed on an electrochemical workstation (BioLogic SP-300) over a frequency range from 100 MHz to 1 Hz.

3. RESULTS AND DISCUSSION

3.1. Synthesis of the P(100%TP-Etlm) Polymer. A diverse array of rigid and ether-free polymers has recently been synthesized via superacid-catalyzed polyhydroxyalkylation reactions involving various ketones and electron-rich aromatic compounds. As previously reported, kinds of polymers with piperidine and pyridine functionalities respectively, were successfully prepared using *N*-methyl-4-piperidone 20,23,24 and 4-acetylpyridine 19,27 as the ketone monomers. In addition to

ketones, certain aldehyde derivatives, bearing electron-with-drawing groups or groups that become electron-withdrawing under acidic conditions, have also been employed in Friedel—Crafts hydroxyalkylation polycondensation. 43–46

Building on this strategy, herein 1-ethyl-2-imidazolecarbaldehyde was selected to react with p-terphenyl to yield a rigid, ether-free polymer featuring ethylimidazole side groups (designated as P(100%TP-EtIm)). The proposed mechanism is illustrated in Figure 2. Under the influence of the strong Brønsted acid TFSA, both the aldehyde and imidazole moieties in 1-ethyl-2-imidazolecarbaldehyde become activated by protonation. The protonated aldehyde rapidly forms a carbocation intermediate (b), which then undergoes electrophilic aromatic substitution with p-terphenyl to generate intermediate (c). This intermediate is further protonated, and upon dehydration, produces a more reactive carbocation species (e). This carbocation subsequently reacts with another p-terphenyl molecule in a similar manner, forming a triphenylmethane-like intermediate (f). Continued reaction with additional activated aldehyde (b) initiates chain propagation, resulting in a polymer containing both rigid p-terphenyl linkages and pendant ethylimidazole groups.

It is important to note that not all aromatic or imidazole-based aldehydes are capable of forming high-molecular-weight polymers with p-terphenyl. In our recent study, ³¹ we investigated reactivity of five different imidazole-functionalized aldehydes with p-terphenyl and found that both the position of the formyl group and the structure of the imidazole ring played

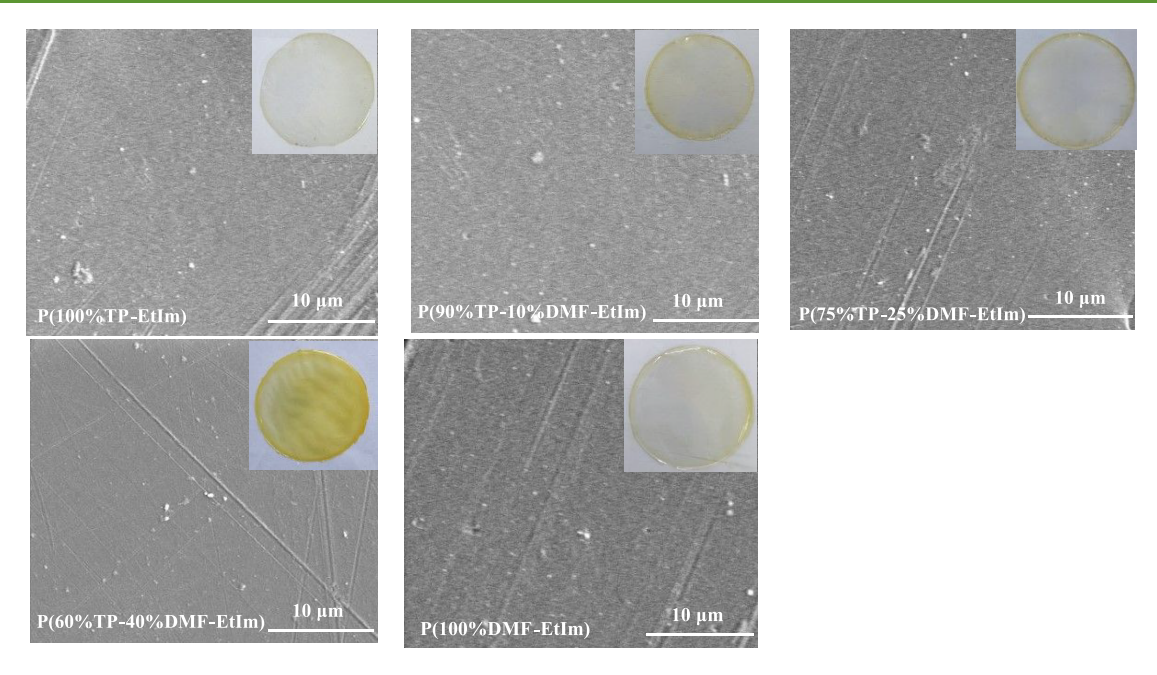


Figure 4. SEM and optical images of P(x%TP-y%DMF-EtIm) membranes.

critical roles in determining their polymerization behavior. Among the aldehydes examined, only 1-methyl-2-imidazolecarboxaldehyde and 1H-imidazole-4-carbaldehyde yielded high-viscosity polymers suitable for the fabrication of mechanically robust membranes. A similar trend has been reported in small-molecule organic synthesis by Klumpp and co-workers, 47-4849 who systematically studied the reactivity of acetyl- and aldehyde-substituted heteroaromatic compounds in superelectrophilic systems. Their findings highlighted the importance of dication formation as a key factor for superelectrophilic activation of imidazole derivatives. In the present study, 1-ethyl-2-imidazolecarbaldehyde demonstrated reactivity comparable to its methyl analogue (i.e., 1-methyl-2imidazolecarbaldehyde) under superacidic conditions, enabling efficient polymerization with p-terphenyl. Notably, 1-ethyl-2imidazolecarbaldehyde offers a distinct cost advantage and its ethyl group may hinder the polymer chain packing, potentially enhancing the free volume and improving PA doping capability. Furthermore, copolymerization with the highly rigid DMF segment was adopted to enhance the backbone rigidity, further disrupt tight chain packing, and increase the polymer's free volume, thereby promoting greater PA uptake and proton conductivity.

3.2. Chemical Structure of Copolymers. The successful synthesis of the P(x%TP-y%DMF-EtIm) copolymers was confirmed through both ¹H NMR and FT-IR spectroscopy. As shown in Figure 3a, the ¹H NMR spectra display distinct signals corresponding to each structural unit. For the homopolymer P(100%TP-EtIm), aromatic protons from the p-terphenyl segments appear in the range of 7.39-7.80 ppm (H_{6-8}) , while the peaks at 7.36 and 7.10 ppm $(H_{3,4})$ are attributed to protons on the imidazole rings. The methine proton (-CH-) within the polymer backbone is observed at 5.97 ppm (H_5) , and the ethyl side group yields signals at 4.03 and 1.17 ppm (H₂ and H₁, respectively). For the homopolymer P(100%DMF-EtIm), a characteristic peak at 1.32 ppm (H_f) corresponds to the methyl protons of the 9,9-dimethylfluorene moiety. 28,38 In the copolymer P(75%TP-25%DMF-EtIm), all expected peaks from the two respective homopolymers are

present, verifying the successful incorporation of p-terphenyl, 9,9-dimethylfluorene, and ethylimidazole segments into the copolymer backbone. Notably, the methine proton signal shows a slight downfield shift to 6.01 ppm compared to 5.97 ppm in P(100%TP-EtIm), possibly due to differences in the electronic environment caused by the introduction of the DMF segments. The relative content of DMF in P(75%TP-25% DMF-EtIm) was estimated by integrating the areas of peaks f (attributed to DMF) against peak 1'+a' (ethylimidazole), using the formula DMF%= $(A_f/6)/(A_{1'+a'}/3)$ The calculated DMF molar fraction was 27.04%, closely matching the theoretical feed ratio, thus confirming effective copolymerization.

The FT-IR spectra (Figure 3b) further corroborate the formation of the copolymers. Characteristic vibrational bands near 3032 and 2970 cm⁻¹ correspond to aromatic and aliphatic C–H stretching, ⁵⁰ respectively. The absorption band around 1590 cm⁻¹ is assigned to the C=N stretching of the imidazole ring, while the peak at 1275 cm⁻¹ corresponds to C–N stretching from the ethylimidazole side group. ⁵¹ A peak at 787 cm⁻¹ is attributed to out-of-plane bending vibrations of aromatic C–H bonds. Together, the ¹H NMR and FT-IR results clearly verify the successful synthesis of the designed P(x%TP-y%DMF-EtIm) copolymers.

Computational simulations based on P(100%DMF-EtIm) and P(100%TP-EtIm) molecular models were conducted as previous described.²⁹ Figure 3c,d shows that P(100%DMF-EtIm) exhibits a higher free volume ratio (27.85%) and a larger accessible 3D surface area compared to P(100%TP-EtIm) (22.05%). This result supports the hypothesis that the introduction of bulky and contorted DMF segments promotes looser chain packing, ^{38,39} thereby increasing accessible free volume and consequently enhancing the PA doping capacity.

3.3. Preparation of Membranes. Imidazole-functionalized, aryl-ether-free copolymers were synthesized via a TFSA and TFA catalyzed Friedel—Crafts hydroxyalkylation between aromatic monomers (*p*-terphenyl and 9,9-dimethylfluorene) and 1-ethyl-2-imidazolecarbaldehyde. Due to the high reactivity of the monomers, ^{18,19} the polymerization proceeded efficiently, affording polymers with sufficient inherent

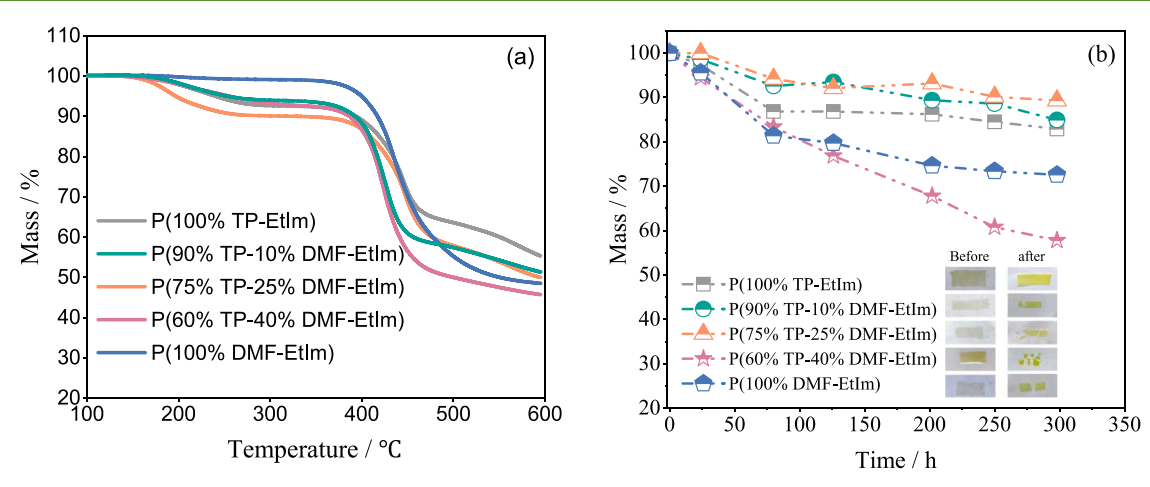


Figure 5. (a) TGA curves under N_2 at a heating rate of 10 °C min⁻¹ and (b) oxidative stability evaluation via Fenton test (3.0 wt % H_2O_2 , 4.0 ppm Fe^{2+} , 80 °C) of P(x%TP-y%DMF-EtIm) membranes.

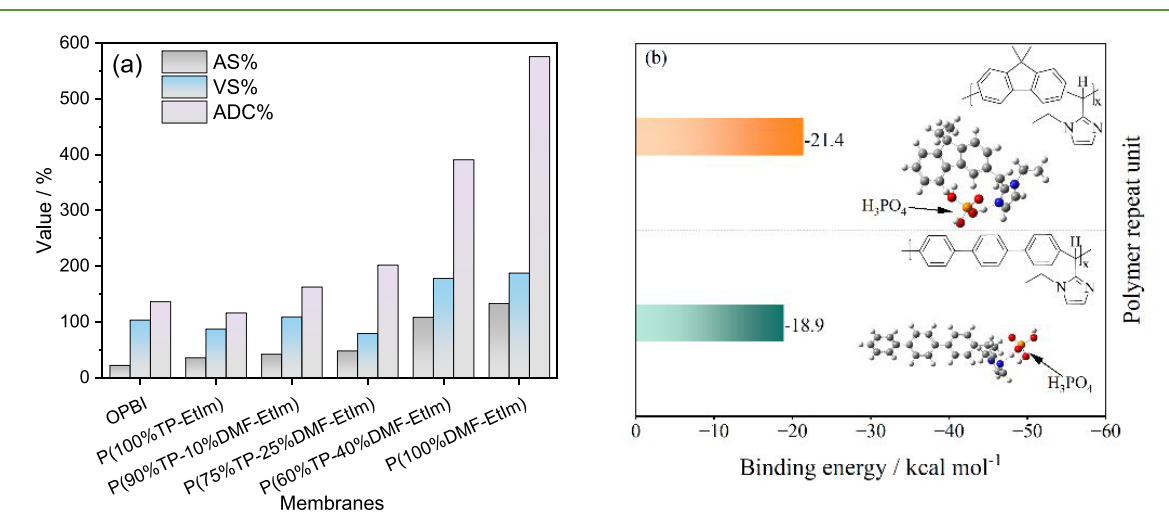


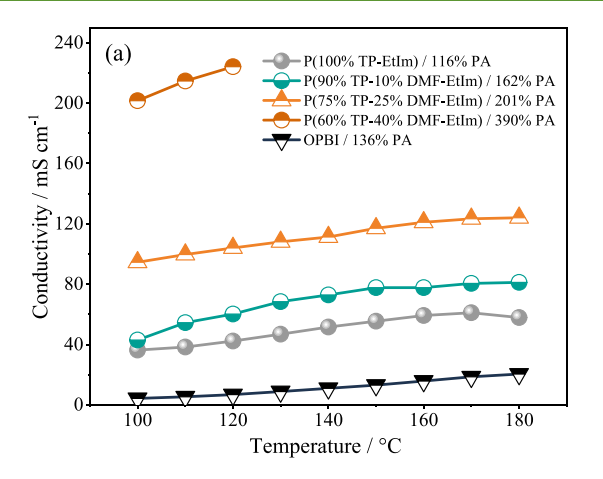
Figure 6. (a) Acid doping content and swelling ratios of various membranes after soaking in 85 wt % PA solutions at 30 °C; (b) binding energies between P(100%TP-EtIm)/P(100%DMF-EtIm) repeat unit and one PA molecule.

viscosities, which were 2.41, 0.59, 2.53, 1.65, and 2.80 dL g⁻¹ for P(100%DMF-EtIm), P(60%TP-40%DMF-EtIm), P(75% TP-25%DMF-EtIm), P(90%TP-10%DMF-EtIm) and P(100% TP-EtIm), respectively. Additionally, GPC analysis was conducted using DMF as the eluent. As listed in Table S1, the M_n of P(75%TP-25%DMF-EtIm) was 62 kDa with dispersity (D) of 2.8, indicating sufficient molecular weight to yield mechanically robust membranes suitable for HT-PEM applications. All polymers, including both homopolymers and P(x%TP-y%DMF-EtIm) copolymers, exhibited excellent solubility in common polar organic solvents such as DMAc, DMF, DMSO, and NMP. This high solubility can be attributed to the presence of tetrahedral sp³-hybridized carbon centers in the polymer backbone, which hinder chain packing and enhance solubility. Membranes were prepared via a simple solution-casting method using DMAc. As shown in Figure 4, the resulting membranes were uniform, transparent, and light yellow in color. SEM imaging confirmed their dense and nonporous microstructure, which is crucial for minimizing gas crossover and achieving higher open circuit voltages (OCVs) in fuel cell applications.

3.4. Thermal and Chemical Stabilities. The thermal stability of the membranes was evaluated by TGA under nitrogen atmosphere (Figure 5a). All P(x%TP-y%DMF-EtIm)

samples exhibited excellent thermal stability, withstanding temperatures up to 250 °C, and showed major decomposition of the polymer backbone only above 410 °C. Notably, P(100% TP-EtIm) and P(75%TP-25%DMF-EtIm) displayed ~8% mass loss between 200 and 300 °C, despite TP-based components accounting for approximately 65 and 50% of their total mass, respectively. This suggests that the observed weight loss is primarily due to the removal of residual crystallized water or terminal groups, rather than backbone degradation. Importantly, all membranes remained stable well above the operational temperature range of HT-PEMFCs (typically below 200 °C), 4,6 confirming their potential for use in HT-PEMFCs.

Chemical stability was assessed via Fenton's test (Figure 5b), which simulates oxidative degradation through the generation of radical species such as ◆OH and ◆OOH. ^{10,23,27} Most degradation occurred within the first 80 h. Among the tested membranes, P(60%TP-40%DMF-EtIm) exhibited the most rapid degradation over a 300-h period, likely due to its relatively low molecular weight (viscosity: 0.59 dL g⁻¹). Other membranes showed significantly improved oxidative stability, with some maintaining structural integrity for up to 300 h. Moreover, ¹H NMR analysis (Figure S1) confirms the chemical structure of P(100%TP-EtIm), P(75%TP-25%



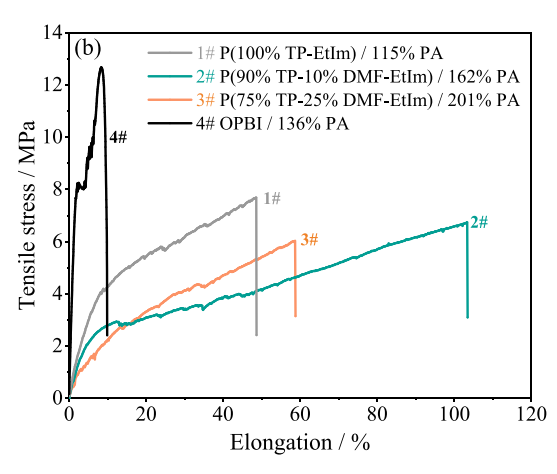


Figure 7. (a) Proton conductivity as a function of temperature and (b) mechanical stress—strain curves at RT of various PA doped P(x%TP-y%DMF-EtIm) membranes.

DMF-EtIm), and P(100%DMF-EtIm) membranes remains intact after 300 h in Fenton's reagent, suggesting strong resistance to radical-induced degradation. This excellent oxidative stability is attributed to the rigid, fully aromatic, ether-free polymer backbone. Additionally, it is also important to note that the discussion above regarding radical stability pertains to pristine membranes and does not consider the inevitable presence of PA, which can significantly affect the outcome of Fenton's tests. PA acts as a chelating agent for metal ions, promoting the precipitation of metal phosphates and thereby reducing the concentration of free metal ions that catalyze radical formation.³ Moreover, PA stabilizes hydrogen peroxide under acidic conditions, further inhibiting radical generation. Acid-base interactions between PA and the nitrogen atoms in imidazole rings may also mitigate radical attack. On the other hand, PA doping can lead to membrane swelling, potentially increasing their vulnerability to oxidative degradation. Overall, the net effect of PA is expected to suppress oxidative degradation of membranes in Fenton's reagent.

3.5. Acid Doping and Swelling. The absorbed PA content significantly influences the proton conductivity and tensile strength of HT-PEMs.^{2,10} As shown in Figure 6a, the acid doping content (ADC%) and dimensional swelling ratios (S% and V%) of various membranes were measured after immersion in 85 wt % PA solution at 30 °C. Due to the presence of pendant and freely rotating ethylimidazole basic groups, the P(100%TP-EtIm) membrane exhibited an ADC% of 116%, which can be attributed to acid-base interactions and hydrogen bonding between the imidazole moieties and PA molecules. 7,31 Moreover, the ADC% of P(x%TP-y%DMF-EtIm) copolymer membranes increased proportionally with the content of 9,9-dimethylfluorene units in the polymer backbone. For example, the ADC% increased markedly from 162 to 390% as the proportion of 9,9-dimethylfluorene increased from 10 to 40%, due to the twisted and bulky structure of dimethylfluorene, which introduces more free volume.^{38,39} Notably, the P(100%DMF-EtIm) membrane became noticeably soft after doping and showed an ADC% exceeding 575%. Thus, to improve the mechanical and dimensional stability, rigid p-terphenyl units need to be copolymerized into the polymer backbone. To further elucidate the interactions between polymer chains and PA, binding energies between a single PA molecule and the

repeating units of P(100%TP-EtIm) and P(100%DMF-EtIm) were calculated, as shown in Figure 6b. The PA-ethylmethylimidazole complex of P(100%DMF-EtIm) displayed a binding energy of 21.4 kcal mol^{-1} , slightly higher than that of P(100%TP-EtIm) (18.9 kcal mol^{-1}), indicating stronger acid—base interactions in the former system. These results affirm the important role of 9,9-dimethylfluorene in enhancing PA uptake.

Generally, a higher PA doping level leads to improved proton conductivity, though it is often accompanied by increased dimensional swelling due to plasticization effects induced by PA. As shown in Figure 6a, the P(60%TP-40% DMF-EtIm) membrane with an ADC% of 390% showed swelling ratios (S% and V%) of 108% and 177%, respectively, i.e., 2.5 and 1.6 times greater than those of P(90%TP-10% DMF-EtIm) (ADC%=162%). The P(100%DMF-EtIm) membrane, with the highest ADC% of 575%, exhibited the largest S% and V% of 133 and 188%, respectively. Thus, optimizing the content of dimethylfluorene in copolymers allows for a favorable balance between high PA doping and acceptable dimensional stability.

3.6. Proton Conductivity and Mechanical Properties. Proton conductivity is a critical parameter for evaluating membrane performance in HT-PEMFCs. 9,10 Figure 7a illustrates the anhydrous proton conductivities of various PAdoped membranes measured from 100 to 180 °C. As expected, conductivity increased with temperature due to accelerated proton transport dynamics. 6,32,35 For instance, the proton conductivity of P(75%TP-25%DMF-EtIm)/201%PA rose from 94 mS cm $^{-1}$ at 100 °C to 124 mS cm $^{-1}$ at 180 °C. Furthermore, increasing the content of dimethylfluorene significantly improved the conductivity due to greater PA uptake, which enhances the hydrogen-bonding network essential for proton hopping via the Grotthuss mechanism.^{3,9,24} As a result, the P(60%TP-40%DMF-EtIm)/390%PA membrane achieved the highest proton conductivity of 224 mS cm⁻¹ at 120 °C, approximately 32 times higher than that of a benchmark OPBI/136%PA membrane (7 mS cm⁻¹ at 120 °C).

Besides conductivity, mechanical robustness is equally important for ensuring membrane durability in fuel cell operation. After PA doping, the P(60%TP-40%DMF-EtIm) membrane became too soft for mechanical testing. Therefore, mechanical properties were evaluated for the other PA-doped membranes. Generally, higher ADC% led to

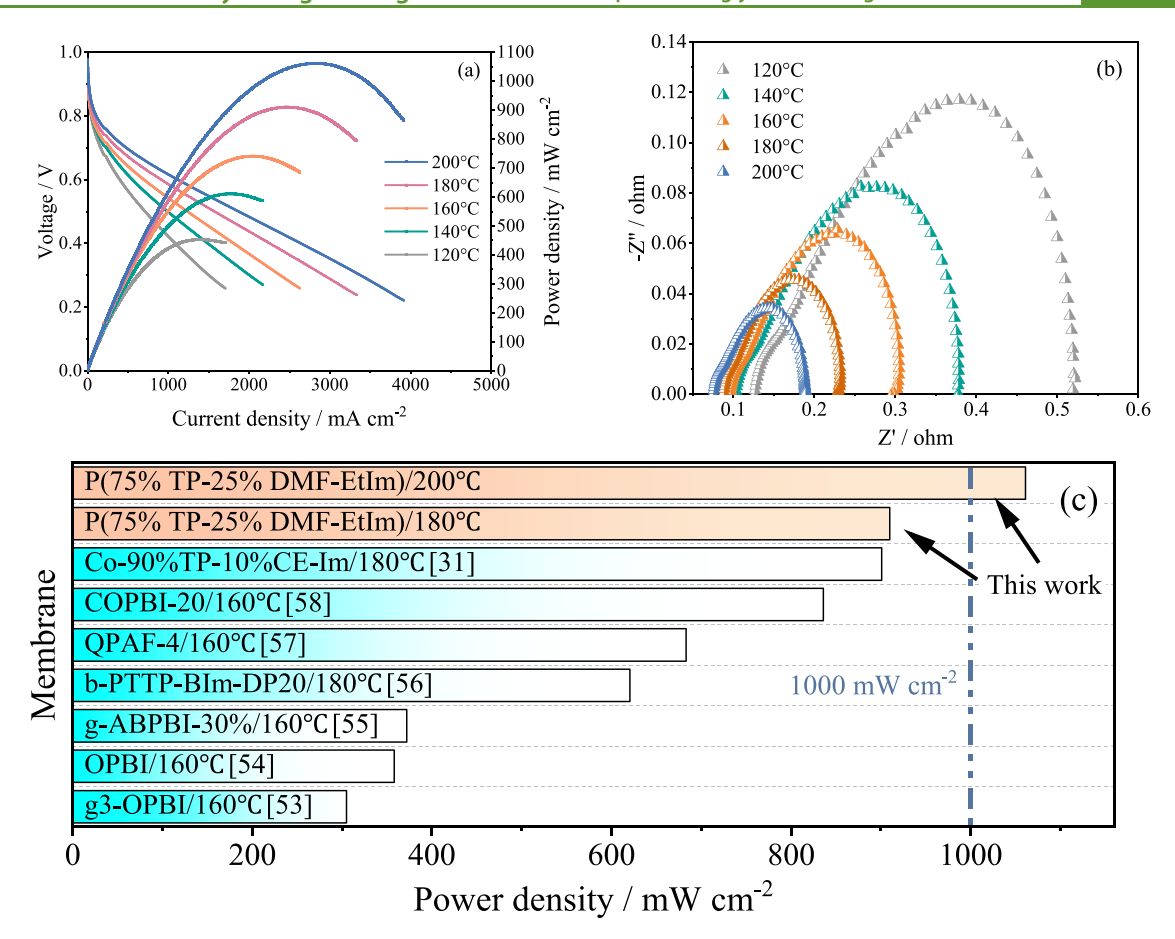


Figure 8. (a) Polarization and power density curves, and (b) electrochemical impedance spectra of the H_2 – O_2 fuel cell based P(75%TP-25%DMF-EtIm)/201%PA (thickness: \sim 80 μ m) without humidification or any backpressure; (c) Comparisons of power density of the H_2 – O_2 cell with P(75% TP-25%DMF-EtIm)/201%PA and other HT-PEMs in the literature.

enhanced conductivity but also compromised mechanical strength due to greater swelling. As shown in Figure 7b, with increasing dimethylfluorene content, the tensile strength gradually declined while the elongation at break increased. Notably, the tensile strengths of P(100%TP-EtIm), P(90%TP-10%DMF-EtIm), and P(75%TP-25%DMF-EtIm) were 7.7, 6.7, and 6.0 MPa, respectively, sufficient to meet the mechanical requirements for HT-PEMFC applications.

3.7. Fuel Cell Performance. Taking the overall performance of the membranes, the P(75%TP-25%DMF-EtIm)/201% PA membrane was chosen to assemble membrane electrode assemble (MEA) and evaluate the H2-O2 HT-PEMFC performance. As shown in Figure 8a, the cell with P(75%TP-25%DMF-EtIm)/201%PA demonstrate outstanding fuel cell performance. In all temperature, the OCVs were above 0.95 V, indicating the good gas isolation performance.³¹ As the temperature rising from 120 to 200 °C, the fuel cell performance gradually improved, with an impressive peak power density of 1060 mW cm⁻² at 200 °C without any backpressure and humidification. As shown in Figure 8b, the electrochemical impedances of the H2-O2 single cell significantly decreased when the temperature increased from 120 to 200 °C. This notable improvement can be attributed to enhanced proton conductivity and improved electrode kinetics at elevated operating temperatures.^{2,3*} In contrast, our group's previously reported OPBI/162%PA membrane achieved a considerably lower peak power density of 437 mW cm⁻² under similar conditions at 180 °C.35 To assess acid retention and

thermal stability, the P(75%TP-25%DMF-EtIm)/201%PA membrane was tested under fuel cell operating conditions (160 °C, 200 mA cm $^{-2}$). As shown in Figure S2, the cell voltage remained nearly unchanged over 70 h, indicating minimal PA loss. It is worth noting, however, that extended durability tests remain essential for fully assessing long-term membrane stability. It is previously reported that the average acid loss rate is estimated to be 2–4 mg $\rm H_3PO_4\,cm^{-2}$ per 10,000 hours of continuous operation for PA doped PBI membranes. The primary mechanism of acid loss is evaporation, which is strongly influenced by variables such as the acid vapor pressure, gas flow rate, and cell temperature. $\rm ^{52}$

As depicted in Figure 8c, the P(75%TP-25%DMF-EtIm)/ 201%PA attained a peak power density of 910 mW cm⁻² at 180 °C, significantly outperforming many previously reported PA-doped HT-PEMs. For comparison, the cell with g3-OPBI and OPBI membrane delivered 305 and 358 mW cm⁻² at 160 °C, 16,53 while the cell with g-ABPBI-30% exhibited 372 mW cm⁻² at the same temperature.⁵⁴ Li et al. developed a new polymer b-PTTP-BIm-DP20,55 which reached a power density of 621 mW cm⁻² at 180 °C. Jiang et al. synthesized QPAF-4 composed of perfluoroalkylene and fluorenyl groups with pendant ammonium groups and achieved 683 mW cm⁻².^{1,12} Pei et al. grafted ethyl imidazole on the side chain of the PBI and blended with OPBI to obtain COPBI-20, which exhibited a power density of 836 mW cm^{-2.56} It is worth noting that HT-PEMFC performance is governed by multiple operational and structural factors, including MEA fabrication protocols, gas

purity, catalyst composition, and three-phase interface. Nevertheless, the results demonstrate the considerable promise of P(75%TP-25%DMF-EtIm)/PA membranes as advanced candidates for HT-PEMFCs.

4. CONCLUSIONS

In this study, a series of poly(terphenyl-co-9,9-dimethylfluorene-ethylimidazole) copolymers was synthesized via a superacid-catalyzed Friedel-Crafts hydroxyalkylation reaction to develop HT-PEMs with balanced physicochemical properties and excellent fuel cell performance. The incorporation of 9,9'dimethylfluorene segments was designed to disrupt polymer chain packing and introduce additional free volume, thereby improving PA uptake. Efficient polymerization was achieved using a low-cost, highly reactive ethylimidazole-based aldehyde monomer (EtIm). By varying the p-terphenyl/9,9-dimethylfluorene ratio, the relationship between polymer structure and membrane performance was systematically investigated. The successful synthesis was confirmed by ¹H NMR and FT-IR spectroscopy, while SEM imaging revealed dense, nonporous membrane morphologies. TGA and Fenton tests demonstrated the membranes' good thermal and oxidative stability. The twisted and bulky dimethylfluorene units contributed to higher free volume, and the resulting PA-EtIm complexes exhibited stronger binding energy, enhancing both acid doping content and proton conductivity. Among the series, P(75%TP-25% DMF-EtIm) achieved an optimal balance between conductivity and mechanical integrity, with a proton conductivity of 124 mS cm⁻¹ at 180 °C and a tensile strength of 6.12 MPa after PA doping. Remarkably, a H₂-O₂ fuel cell using the P(75%TP-25%DMF-EtIm)/201%PA membrane delivered a peak power density of 1060 mW cm⁻² at 200 °C under dry, nonpressurized conditions. Overall, this work demonstrates the effectiveness of integrating dimethylfluorene units into HT-PEMs and offers a promising design strategy for advanced polymer electrolytes in HT-PEMFC applications.

ASSOCIATED CONTENT

Supporting Information

The Supporting Information is available free of charge at https://pubs.acs.org/doi/10.1021/acssuschemeng.5c06214.

¹H NMR spectra of membranes after Fenton test for 300 h; fuel cell durability at 200 mA cm⁻² and 160 °C; number-average molecular weight; comparisons of peak power densities of various membranes (PDF)

AUTHOR INFORMATION

Corresponding Authors

Jin Wang — School of Pharmacy, Shenyang Medical College, Shenyang 110034, China; Email: wangjin@symc.edu.cn Jingshuai Yang — Department of Chemistry, College of Sciences, Northeastern University, Shenyang 110819, China; orcid.org/0000-0002-0275-0978; Email: yjs@mail.neu.edu.cn

Authors

Lei Li — Department of Chemistry, College of Sciences, Northeastern University, Shenyang 110819, China Qi Liao — Department of Chemistry, College of Sciences, Northeastern University, Shenyang 110819, China Ruixuan Lv — Department of Chemistry, College of Sciences, Northeastern University, Shenyang 110819, China Lele Wang – Department of Chemistry, College of Sciences, Northeastern University, Shenyang 110819, China Lili Sui – School of Pharmacy, Shenyang Medical College, Shenyang 110034, China

Complete contact information is available at: https://pubs.acs.org/10.1021/acssuschemeng.5c06214

Author Contributions

The manuscript was written through contributions of all authors.

Notes

The authors declare no competing financial interest.

ACKNOWLEDGMENTS

We gratefully acknowledge the Science and Technology Major Project of Liaoning Province (Grant No. 2024JH1/11700015), Natural Science Foundation of China (52403273) and Zhejiang TUNA Environmental Science & Technology Limited Company (2024020600001) for financially supporting this work. We would like to express our gratitude to prof. J.G. Liu from Institute of Metal Research, Chinese Academy of Sciences for the assistance with the theoretical calculations.

REFERENCES

- (1) Haider, R.; Wen, Y.; Ma, Z.-F.; Wilkinson, D. P.; Zhang, L.; Yuan, X.; Song, S.; Zhang, J. High temperature proton exchange membrane fuel cells: progress in advanced materials and key technologies. *Chem. Soc. Rev.* **2021**, *50*, 1138–1187.
- (2) Song, J.; Zhao, W.; Zhou, L.; Meng, H.; Wang, H.; Guan, P.; Li, M.; Zou, Y.; Feng, W.; Zhang, M.; Zhu, L.; He, P.; Liu, F.; Zhang, Y. Rational materials and structure design for improving the performance and durability of high temperature proton exchange membranes (HT-PEMs). *Adv. Sci.* **2023**, *10*, No. 2303969.
- (3) Aili, D.; Henkensmeier, D.; Martin, S.; Singh, B.; Hu, Y.; Jensen, J. O.; Cleemann, L. N.; Li, Q. Polybenzimidazole-based high-temperature polymer electrolyte membrane fuel cells: new insights and recent progress. *Electrochem. Energy Rev.* **2020**, *3*, 793–845.
- (4) Jung, J.; Kim, J.; Park, S. Y.; Ahn, C.-H.; Lee, J.-H.; Seo, S. H.; Lee, A. S. Advances in ion conducting membranes and binders for high temperature polymer electrolyte membrane fuel cells. *Polym. Rev.* **2022**, *62*, 789–825.
- (5) Hu, M.; Li, T.; Neelakandan, S.; Wang, L.; Chen, Y. Cross-linked polybenzimidazoles containing hyperbranched cross-linkers and quaternary ammoniums as high-temperature proton exchange membranes: enhanced stability and conductivity. *J. Membr. Sci.* **2020**, 593, No. 117435.
- (6) Murdock, L. A.; Benicewicz, B. C. Teaching an Old Dog New Tricks: Synthesis, Processing, and Application of Polybenzimidazole (PBI) Membranes. *ACS Appl. Energy Mater.* **2024**, *7*, 239–249.
- (7) You, X.; Ju, Q.; Ma, Y.; Yi, G.; Jiang, Z.; Li, N.; Zhang, Q. High conductivity poly(meta-terphenyl alkylene)s proton exchange membranes for high temperature fuel cell. *Chem. Eng. J.* **2024**, 487, No. 150535.
- (8) Dong, Y.; Zhong, S.; He, Y.; Liu, Z.; Zhou, S.; Li, Q.; Pang, Y.; Xie, H.; Ji, Y.; Liu, Y.; Han, J.; He, W. Modification strategies for non-aqueous, highly proton-conductive benzimidazole-based high-temperature proton exchange membranes. *Chin. Chem. Lett.* **2024**, 35, No. 109261.
- (9) Ma, Y. L.; Wainright, J. S.; Litt, M. H.; Savinell, R. F. Conductivity of PBI membranes for high-temperature polymer electrolyte fuel cells. *J. Electrochem. Soc.* **2004**, *151*, A8–A16.
- (10) Aili, D.; Yang, J.; Jankova, K.; Henkensmeier, D.; Li, Q. From polybenzimidazoles to polybenzimidazoliums and polybenzimidazolides. *J. Mater. Chem. A* **2020**, *8*, 12854–12886.
- (11) Liu, R.; Wang, J.; Che, X.; Wang, T.; Aili, D.; Li, Q.; Yang, J. Facile synthesis and properties of poly(ether ketone cardo)s bearing

- heterocycle groups for high temperature polymer electrolyte membrane fuel cells. J. Membr. Sci. 2021, 636, No. 119584.
- (12) Jiang, J.; Li, Z.; Xiao, M.; Wang, S.; Miyatake, K.; Meng, Y. Quaternary ammonium-biphosphate ion-pair based copolymers with continuous H⁺ transport channels for high-temperature proton exchange membrane. *J. Membr. Sci.* **2022**, *660*, No. 120878.
- (13) Gao, Y.; Mu, T.; Hu, X.; Pang, Y.; Zhao, C. Facile synthesis of all-carbon fluorinated backbone polymers containing sulfide linkage as proton exchange membranes for fuel cells. *Chin. Chem. Lett.* **2025**, *36*, No. 110763.
- (14) Guan, X.; Wu, W.; Zhang, S.; Ma, G.; Zhou, X.; Li, C.; Yu, D.; Luo, Y.; Wang, S. High hydrogen-bond density polymeric ionic liquid composited high temperature proton exchange membrane with exceptional long-term fuel cell performance. *J. Membr. Sci.* **2025**, 717, No. 123523.
- (15) Wang, B.; Ling, Z.; Liu, Y.; Hu, S.; Liu, Q.; Fu, X.; Zhang, R.; Hu, S.; Zhao, F.; Li, X.; Bao, X.; Yang, J. Side-chain vertical imidazole backbone enhances phosphoric acid uptake in Poly(2,5-benzimidazole) membranes for high-temperature PEMFCs. *Int. J. Hydrogen Energy* **2024**, *84*, 959–967.
- (16) Xiao, Y.; Wang, S.; Tian, G.; Xiang, J.; Zhang, L.; Cheng, P.; Zhang, J.; Tang, N. Preparation and molecular simulation of grafted polybenzimidazoles containing benzimidazole type side pendant as high-temperature proton exchange membranes. *J. Membr. Sci.* 2021, 620, No. 118858.
- (17) Tang, H.; Geng, K.; Hao, J.; Zhang, X.; Shao, Z.; Li, N. Properties and stability of quaternary ammonium-biphosphate ion-pair poly(sulfone)s high temperature proton exchange membranes for $\rm H_2/O_2$ fuel cells. *J. Power Sources* **2020**, 475, No. 228521.
- (18) Olvera, L. I.; Guzmán-Gutiérrez, M. T.; Zolotukhin, M. G.; Fomine, S.; Cárdenas, J.; Ruiz-Trevino, F. A.; Villers, D.; Ezquerra, T. A.; Prokhorov, E. Novel High molecular weight aromatic fluorinated polymers from one-pot, metal-free step polymerizations. *Macromolecules* **2013**, *46*, 7245–7256.
- (19) Cetina-Mancilla, E.; Olvera, L. I.; Balmaseda, J.; Forster, M.; Ruiz-Treviño, F. A.; Cárdenas, J.; Vivaldo-Lima, E.; Zolotukhin, M. G. Well-defined, linear, wholly aromatic polymers with controlled content and position of pyridine moieties in macromolecules from one-pot, room temperature, metal-free step-polymerizations. *Polym. Chem.* **2020**, *11* (38), 6194–6205.
- (20) Olsson, J. S.; Pham, T. H.; Jannasch, P. Poly (arylene piperidinium) hydroxide ion exchange membranes: synthesis, alkaline stability, and conductivity. *Adv. Funct. Mater.* **2018**, 28 (2), No. 1702758.
- (21) Peng, H.; Li, Q.; Hu, M.; Xiao, L.; Lu, J.; Zhuang, L. Alkaline polymer electrolyte fuel cells stably working at 80°C. *J. Power Sources* **2018**, 390, 165–167.
- (22) Wang, J.; Zhao, Y.; Setzler, B. P.; Rojas-Carbonell, S.; Ben Yehuda, C.; Amel, A.; Page, M.; Wang, L.; Hu, K.; Shi, L.; Gottesfeld, S.; Xu, B.; Yan, Y. Poly(aryl piperidinium) membranes and ionomers for hydroxide exchange membrane fuel cells. *Nat. Energy* **2019**, *4*, 392–398.
- (23) Bai, H.; Peng, H.; Xiang, Y.; Zhang, J.; Wang, H.; Lu, S.; Zhuang, L. Poly(arylene piperidine)s with phosphoric acid doping as high temperature polymer electrolyte membrane for durable, high-performance fuel cells. *J. Power Sources* **2019**, 443, No. 227219.
- (24) Jin, Y.; Wang, T.; Che, X.; Dong, J.; Liu, R.; Yang, J. New high-performance bulky *N*-heterocyclic group functionalized poly (terphenyl piperidinium) membranes for HT-PEMFC applications. *J. Membr. Sci.* **2022**, *641*, No. 119884.
- (25) Che, X.; Wang, L.; Wang, T.; Dong, J.; Yang, J. The effect of grafted alkyl side chains on the properties of poly (terphenyl piperidinium) based high temperature proton exchange membranes. *Ind. Chem. Mater.* **2023**, *1*, 516–525.
- (26) Jin, Y.; Wang, T.; Che, X.; Dong, J.; Li, Q.; Yang, J. Poly (arylene pyridine)s: new alternative materials for high temperature polymer electrolyte fuel cells. *J. Power Sources* **2022**, *526*, No. 231131. (27) Lv, R.; Jin, S.; Li, L.; Wang, Q.; Wang, L.; Wang, J.; Yang, J. The influence of comonomer structure on properties of poly(aromatic

- pyridine) copolymer membranes for HT-PEMFCs. J. Membr. Sci. 2024, 701, No. 122703.
- (28) Shi, N.; Wang, G.; Wang, Q.; Wang, L.; Li, Q.; Yang, J. Acid doped branched poly(biphenyl pyridine) membranes for high temperature proton exchange membrane fuel cells and vanadium redox flow batteries. *Chem. Eng. J.* **2024**, *489*, No. 151121.
- (29) Wang, Q.; Zhao, S.; Guo, Y.; Wei, W.; Wang, L.; Yang, J. High-performance poly(aromatic pyridine) copolymers with crown ether moieties for high temperature polymer electrolyte membrane fuel cells. *Sci. China Chem.* **2025**, *68*, 1078–1090.
- (30) Wang, Q.; Zhang, Z.; Lv, P.; Peng, Z.; Yang, J. Poly(terphenyl pyridine) based amphoteric and anion exchange membranes with high ionic selectivity for vanadium redox flow batteries. *Chem. Eng. J.* **2025**, *505*, No. 58922.
- (31) Mu, T.; Wang, L.; Wang, Q.; Wu, Y.; Jannasch, P.; Yang, J. High-performance imidazole-containing polymers for applications in high temperature polymer electrolyte membrane fuel cells. *J. Energy Chem.* **2024**, *98*, 512–523.
- (32) Wang, L.; Wang, Q.; Lv, P.; Peng, Z.; Yang, J. Synthesis of poly(terphenyl-co-dibenzo-18-crown-6 methylimidazole) copolymers for high-performance high temperature polymer electrolyte membrane fuel cells. *J. Membr. Sci.* 2025, 714, No. 123416.
- (33) Wang, L.; Celenk, S.; Wang, Q.; Li, Q.; Yang, J. Long-durability poly(dibenzofuran-co-terphenyl N-methylimidazole) copolymer membranes for high-temperature polymer electrolyte membrane fuel cells. *Macromolecules* **2025**, *58*, 5344–5355.
- (34) Wang, Q.; Sang, L.; Huang, L.; Guan, J.; Yu, H.; Zheng, J.; Zhang, Q.; Qin, G.; Li, S.; Zhang, S. Design and synthesis of comblike bisulfonic acid proton exchange membrane with regulated microstructure. *Adv. Funct. Mater.* **2024**, 34, No. 2316506.
- (35) Wang, Q.; Wang, L.; Zhang, M.; Peng, Z.; Lu, Y.; Lv, P.; Yang, J. Preparation of novel membranes with multiple hydrogen bonding sites and π -conjugated structure for high temperature proton exchange membrane fuel cells. *Chem. Commun.* **2024**, *60* (40), 5318–5321.
- (36) Lai, L. W.; Yue, X. B.; Liu, Y. J.; Wang, X. H.; Peng, H.; Zhang, G. L.; Hu, Y. Q.; Zhang, Q. G.; Zhu, A. M.; Liu, Q. L. Tuning poly(isatin biphenyl) anion exchange membranes by copolymerization and branching. *J. Membr. Sci.* **2024**, *710*, No. 123157.
- (37) Wang, Q.; Wei, T.; Peng, Z.; Zhao, Y.; Jannasch, P.; Yang, J. High-performance anion exchange membranes based on poly-(oxindole benzofuran dibenzo-18-crown-6)s functionalized with hydroxyl and quaternary ammonium groups for alkaline water electrolysis. *J. Colloid Interface Sci.* **2025**, *686*, 304–317.
- (38) Chen, N.; Wang, H. H.; Kim, S. P.; Kim, H. M.; Lee, W. H.; Hu, C.; Bae, J. Y.; Sim, E. S.; Chung, Y.-C.; Jang, J.-H.; Yoo, S. J.; Zhuang, Y.; Lee, Y. M. Poly(fluorenyl aryl piperidinium) membranes and ionomers for anion exchange membrane fuel cells. *Nat. Commun.* **2021**, *12*, No. 2367.
- (39) Lim, H.; Jeong, J.-Y.; Lee, D. H.; Myeong, S.-W.; Shin, G.; Choi, D.; Kim, W. B.; Choi, S. M.; Park, T. Morphology and cell performance of poly(fluorene)-based anion exchange membranes for water electrolysis: effect of backbone core structure. *J. Mater. Chem. A* **2023**, *11*, 25938–25944.
- (40) Li, J.; Li, X.; Zhao, Y.; Lu, W.; Shao, Z.; Yi, B. Hightemperature proton-exchange-membrane fuel cells using an ether-containing polybenzimidazole membrane as electrolyte. *ChemSusChem* **2012**, *5*, 896–900.
- (41) Li, T.; Chai, S.; Liu, B.; Zhao, C.; Li, H. All-carbon backbone aromatic polymers for proton exchange membranes. *J. Polym. Sci.* **2023**, *61*, 2796–2814.
- (42) Wang, L.; Wang, Q.; Li, L.; Lv, R.; Jin, S.; Yang, J.Progress in high-performance high temperature proton exchange membranes for fuel cells *Ion Exchange Adsorpt.* 2024; Vol. 40, pp 366–375.
- (43) Zou, L.; Cao, X.; Zhang, Q.; Dodds, M.; Guo, R.; Gao, H. Friedel-Crafts A2 + B4 polycondensation toward regioselective linear polymer with rigid triphenylmethane backbone and its property as gas separation membrane. *Macromolecules* **2018**, *51*, 6580–6586.

- (44) Weng, Y.; Li, Q.; Li, J.; Gao, Z.; Zou, L.; Ma, X. Facile synthesis of bi-functionalized intrinsic microporous polymer with fully carbon backbone for gas separation application. *Sep. Purif. Technol.* **2021**, 279, No. 119681.
- (45) Zhou, S.; Guan, J.; Li, Z.; Zhang, Q.; Zheng, J.; Li, S.; Zhang, S. Synthesis of fluorinated poly(phenyl-alkane)s of intrinsic microporosity by regioselective aldehyde (A2) + aromatics (B2) Friedel-Crafts polycondensation. *Macromolecules* **2021**, *54*, 6543–6551.
- (46) Yin, L.; Ren, R.; He, L.; Lee, H.; Zhang, Q.; Ding, G.; Wang, L.; Sun, L. Polyarylmethylpiperidinium (PAMP) for next generation anion exchange membranes. *Angew. Chem., Int. Ed.* **2025**, *64*, No. e202503715.
- (47) Klumpp, D. A.; Garza, M.; Sanchez, G. V.; Lau, S.; de Leon, S. Electrophilic activation of acetyl-substituted heteroaromatic compounds. *J. Org. Chem.* **2000**, *65*, 8997–9000.
- (48) Vuong, H.; Stentzel, M.; Klumpp, D. Superacid-promoted synthesis of quinoline derivatives. *Tetrahedron Lett.* **2020**, *61*, No. 151630.
- (49) Sheets, M. R.; Li, A.; Bower, E.; Weigel, A.; Abbott, M.; Gallo, R.; Mitton, A.; Klumpp, D. Superelectrophilic chemistry of imidazoles. *J. Org. Chem.* **2009**, *74*, 2502–2507.
- (50) Liu, B.; Duan, Y.; Li, T.; Pang, Y.; Liu, Q.; Li, Q.; Hu, X.; Zhao, C. Poly(triphenylene-piperidine) membranes reinforced by carboxy intrinsic microporous polymers towards high output power at low phosphoric acid levels for HT-PEMFC. *J. Membr. Sci.* **2024**, 692, No. 122273.
- (51) Ju, M.; Ren, Q.; Xu, J.; Chen, X.; Meng, L.; Lei, J.; Zhao, P.; Wang, Z. Construction of alkali-stable anion exchange membranes with hydrophilic/hydrophobic microphase separation structure by adjusting side chain length. *Chem. Eng. J.* **2023**, *466*, No. 143023.
- (52) Seselj, N.; Aili, D.; Celenk, S.; Cleemann, L. N.; Hjuler, H. A.; Jensen, J. O.; Azizi, K.; Li, Q. Performance degradation and mitigation of high temperature polybenzimidazole-based polymer electrolyte membrane fuel cells. *Chem. Soc. Rev.* **2023**, 52 (12), 4046–4070.
- (53) Wu, A.; Liu, J.; Huang, J.; Min, Y.; Wang, Y.; Wang, S.; Wang, L. Constructing high-density hydrogen bonding networks via introducing the bipyridine group for high-performance fuel cell proton exchange membranes. ACS Appl. Energy Mater. 2022, 5, 11815–11824.
- (54) Wang, B.; Ling, Z.; Liu, Y.; Hu, S.; Liu, Q.; Fu, X.; Zhang, R.; Hu, S.; Zhao, F.; Li, X.; Bao, X.; Yang, J. Side-chain vertical imidazole backbone enhances phosphoric acid uptake in poly(2,5-benzimidazole) membranes for high-temperature PEMFCs. *Int. J. Hydrogen Energy* **2024**, 84, 959–967.
- (55) Li, Y.; Xu, Z.; Shi, W.; Wang, M.; Lin, Z.; He, D.; Pan, Y.; Liao, J.; Ang, E. H.; Shen, J. Branched poly(terphenyl trifluoroacetophenone piperidone) membranes with dual-proton conductor assist for enhancing fuel cell performance operation in high-temperature. *J. Membr. Sci.* 2025, 727, No. 124127.
- (56) Pei, Q.; Liu, J.; Wu, H.; Wang, W.; Ji, J.; Li, K.; Gong, C.; Wang, L. Nitrogen dense distributions of imidazole grafted dipyridyl polybenzimidazole for a high temperature proton exchange membrane. *Polymers* **2022**, *14*, No. 2621.

